

## Hyperpolarized gases in magnetic resonance: a new tool for functional imaging of the lung

Klaus Markstaller, W. Schreiber, H.-U. Kauczor

### Angaben zur Veröffentlichung / Publication details:

Markstaller, Klaus, W. Schreiber, and H.-U. Kauczor. 2001. "Hyperpolarized gases in magnetic resonance: a new tool for functional imaging of the lung." *Swiss Medical Weekly*, no. 3536: 503–9. <https://doi.org/10.4414/smw.2001.09776>.

# Hyperpolarised gases in magnetic resonance: a new tool for functional imaging of the lung<sup>1</sup>

Balthasar Eberle, Klaus Markstaller, Wolfgang G. Schreiber, Hans-Ulrich Kauczor

Departments of Anaesthesiology and Radiology, Johannes Gutenberg University, Mainz, Germany

<sup>1</sup> Support: Deutsche Forschungsgemeinschaft DFG Grant TH 315-8; Körber-Stiftung, Hamburg, Germany; Institutional MAIFOR Grant, Johannes Gutenberg University, Mainz; Max-Planck-Gesellschaft, München; Alexander-von-Humboldt Stiftung, Bonn; Research Grant, Nycomed Amersham plc, UK

## Summary

In magnetic resonance imaging (MRI), nuclear spins are the source of the image signal. In the lung, low-proton spin density in alveolar gas and abundant gas-tissue interfaces substantially impair conventional native <sup>1</sup>H-MRI. Spin polarisation can be increased in two non-radioactive noble gas isotopes, <sup>3</sup>He and <sup>129</sup>Xe, by exposure to polarised laser light. When inhaled, such “magnetized” gases provide high-intensity MR images of the pulmonary airspaces. Thus, hyperpolarised gas (HPG) MRI opens up new routes to a) morphologic imaging of airways and alveolar spaces, and b) analysis of the intrapulmonary distribution of inhaled aliquots of these tracer gases; c) diffusion-sensitive MRI-techniques allow mapping of the “apparent diffusion coefficient” (ADC) of <sup>3</sup>He within lung airspaces, where ADC is physically related to local bronchoalveolar dimensions; d) also, <sup>3</sup>He magnetisation decays in an oxygen-containing atmosphere at a rate proportional to ambient PO<sub>2</sub>. This property allows image-based determination of regional broncho-alveolar PO<sub>2</sub> and its decrease

during a breathhold. Currently, these modalities of functional lung imaging are being assessed by several European and American research groups in animal models, human volunteers and patients. First results show good imaging quality with excellent spatial and unprecedented temporal resolution, and attest to the reproducibility, feasibility and safety of the technique. Regionally impaired ventilation of both structural and functional origin is detected with high sensitivity, e.g. in smokers, asthmatics, patients with COPD or after lung transplantation. Studies into regional ADC and PO<sub>2</sub> measurement demonstrate good agreement with reference methods and physiological predictions. The present limitations of HPG-MRI include the HPG production rate and the US and EU health authorities’ still pending final approval for clinical use.

*Key words: helium; xenon; hyperpolarised gases; magnetic resonance imaging; pulmonary ventilation; gas exchange*

## Background

Magnetic resonance imaging of the lung using hyperpolarised noble gases is an emerging methodology for both static imaging of airspace morphology and image-based dynamic and/or regional assessment of pulmonary function. Conventional methods of lung function testing, e.g. spirometry, body plethysmography, and respiratory and blood gas analysis, provide information on global pulmonary function only. Inert gas wash-in or wash-out techniques and the multiple inert gas elimination technique (MIGET) discriminate between two or more functional pulmonary compartments, but cannot spatially allocate them to specific lung regions. Ventilation-perfusion scintigraphy or

SPECT does provide functional information on defined lung regions, but at the expense of radiation exposure and with very limited spatial and temporal resolution. Finally, high-resolution computed tomography yields excellent data on lung morphology and even, with fast imaging software, on the dynamics of aeration; ventilation and gas exchange data, however, must be deduced indirectly [1, 2].

For the – otherwise quite versatile – methodology of proton (<sup>1</sup>H)-MRI, i.e. conventional MRI, access to the lung is hampered by two very fundamental problems: first, <sup>1</sup>H spin density, as the “MR imaging agent”, is prohibitively low within

the  $N_2/O_2/CO_2/H_2O$  atmosphere in airways and alveoli, and second, the vast number of gas-tissue interfaces creates magnetic field inhomogeneities. Native  $^1H$ -MR lung images are thus simply of little practical use. At this juncture, a very fruitful crosstalk between physicists and radiologists from Princeton University and SUNY at Stony Brook, NY, in 1993 led to the development of techniques to artificially enhance spin polarization, and hence MR signal intensity, within the lung airspaces. Since the sixties, nuclear physicists in neutron research have been developing the techniques of so-called hyperpolarisation – or, somewhat more simply, magnetisation – of particular noble gas iso-

topes by “optical pumping” with circularly polarised laser light [3]. Thus magnetised by a factor of  $10^5$  beyond the normal thermal equilibrium, inhaled  $^{129}Xe$  or  $^3He$  became visible in MR images taken with appropriately tuned coils. Albert and Happer were the first to generate  $^{129}Xe$  images of an excised mouse lung [4]. First human applications of optically magnetised  $^3He$  for lung imaging were published by MacFall, Kauczor, and Ebert [5–7]. Since 1997, numerous patient studies have been performed or are still under way to explore the potential of morphologic and functional  $^3He$  MRI [8–11].

## Material and methods

Both  $^{129}Xe$  and  $^3He$  are chemically inert, non-radioactive, non-toxic noble gas isotopes. Xenon's diffusibility within the alveolar space is low, its tissue solubility is high and it is quite lipophilic. These properties lead to clinically relevant absorption of inspired Xe into the blood, and to further distribution into well-perfused organs, i.e. brain and myocardium. The atmospheric, naturally abundant mixture of Xe isotopes, which contains  $\approx 26\%$   $^{129}Xe$ , is readily available, whereas enriched (70%)  $^{129}Xe$  is more expensive.

Xenon is already in current clinical use, e.g. in nuclear medicine for cerebral blood flow studies and ventilation scintigraphy ( $^{133}Xe$ ), for inhalational anaesthesia and as a gaseous CT contrast agent. Despite its chemical inertness, Xe exerts relevant anaesthetic and analgesic actions, and even subanaesthetic concentrations may already elicit nausea and vomiting. For NMR applications,  $^{129}Xe$  has a nuclear magnetic moment (which determines the attainable signal-to-noise ratio) of the order of  $1/3$  that of  $^3He$ ; the degree of polarisation attainable at present is  $\sim 20\%$ . This, however, limits the signal intensity required for MR imaging.

$^3He$ , on the other hand, is a very rare isotope (1.3 ppm of the already rare atmospheric He, or as a byproduct of tritium decay), and more expensive ( $\sim 150$  USD/L at present). It has negligible solubility and absorption, but is highly diffusible. Its physicochemically similar isotope  $^4He$  has long been in clinical use (pulmonary function testing, anaesthesia, diving) and has no systemic adverse effects unless used in hypoxic mixtures. Since the magnetic moment of  $^3He$  and attainable signal-to-noise ratios exceed those of  $^{129}Xe$ , and since  $^3He$  can be polarised to up to 50%, this noble gas is much more suitable for pulmonary MRI studies. The rest of this review, therefore, will chiefly cover research and development in the  $^3He$  field and will only briefly discuss the potential, advantages and disadvantages of  $^{129}Xe$  MRI.

Hyperpolarisation of  $^3He$  and  $^{129}Xe$  can be carried out by indirect (for  $^3He$  and  $^{129}Xe$ ) or direct ( $^3He$  only) optical pumping with circularly polarised laser light. The former, i.e. the indirect polarisation method, involves alkali metals by using spin exchange between, for example, optically pumped Rb vapour and the noble gas to be polarised (spin exchange technique) [3]. This point is of some significance for clinical use, since toxic alkali metal traces must be removed completely from the hyperpolarised noble gas prior to any biological application. The latter method of direct optical pumping is based upon metastability exchange with optically pumped metastable  $^3He$  atoms (metastability exchange technique), and so the alkali metal problem does not arise; this is also the preferred method at the Mainz Physics Institute. Hyperpolarisation grades of 25–45% are obtained reproducibly. Magnetisation is preserved during storage and transport within iron-depleted glass cells and magnetic holding fields.

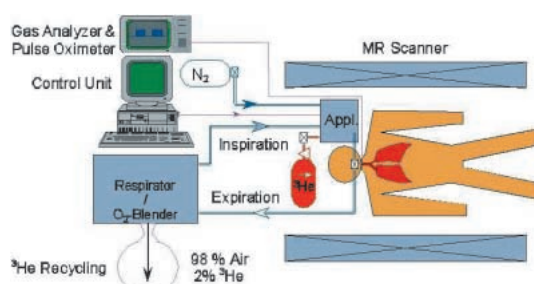
Imaging is performed in a conventional 1.5 T MR scanner (Siemens Magnetom® Vision) equipped with a broad-band amplifier and a transmit-receive coil tuned to the resonance frequency of  $^3He$  at 48.4 MHz. Gas dosage and administration are either by inhalation from prefilled collapsible bags (Tedlar®) or using a self-developed PC-controlled applicator device. Connected to a respirator machine (Servo® 900C, Siemens-Elema), the applicator device allows administration of  $^3He$  and, if required, supplemental oxygen during spontaneous respiration or assisted or controlled ventilation (figure 1). A typical  $^3He$  dose of 200–300 mL is inhaled during a single breath through a nasal continuous positive airway pressure (CPAP) mask, while the patient is monitored (respiratory flows and volumes, respiratory gases, and pulse oximetry). Supplemental  $O_2$ , inspiratory pressure support or CPAP can be provided for. Duration of a typical study is currently 40 min.

In the resultant  $^3He$  images of the lungs, signal intensity is determined by the following principal factors:

- the amount of inhaled polarisation ( $^3He$  volume  $\times$  magnetisation grade);
- loss of magnetisation due to imaging pulses;
- convective distribution and dilution of  $^3He$  in the lung airspaces;
- diffusion of  $^3He$  within the airspaces;
- loss of magnetisation due to paramagnetic  $O_2$ ;
- expiration.

**Figure 1**

Setup for human  $^3He$  MRI studies (Appl: device for  $^3He$  dosage and administration).



In the methodological development of  $^3\text{He}$  MRI our general aim is either to control these variables or utilise them for image-based analysis of regional lung function.

### Objectives

The main objectives of our group's and others' endeavours are at present:

- a. static  $^3\text{He}$  imaging of pulmonary airspace morphology; this is done during one breathhold, using "two-dimensional fast low-angle shot" imaging (2D-FLASH sequences) of adjacent lung slices.
- b. dynamic analysis of regional ventilation distribution; this technique uses fast repetitive slice-selective or projection imaging covering several respiratory cycles. Typical imaging intervals are of the order of 130 ms down to 30 ms.

- c. analysis of  $^3\text{He}$  diffusivity within the restricted airway geometries. Imaging sequences sensitive to the movement of  $^3\text{He}$  atoms are employed. An "apparent diffusion coefficient" (ADC) of  $^3\text{He}$  can be determined which depends, *inter alia*, on airway size.
- d. measurement of regional alveolar partial pressure of oxygen ( $\text{PO}_2$ ). Since molecular  $\text{O}_2$  is paramagnetic, it reduces the magnetisation of  $^3\text{He}$  at a rate which is proportional to  $\text{PO}_2$  [12]. The kinetics of signal decay are obtained from serial FLASH images acquired during one or two breathholds. The contribution of the  $\text{PO}_2$  effect to the total signal decay rate is isolated from that of the imaging process (which in itself destroys magnetisation too) and quantified.

## Results

All studies in healthy volunteers and patients were performed in accordance with the principles of the Declaration of Helsinki, with the approval of the Ethics Committee of the Landesärztekammer Rheinland-Pfalz, and after obtaining the subjects' informed consent. Table 1 summarises volunteer and patient studies performed in Mainz up to 2000.

### Initial $^3\text{He}$ MRI experience in human subjects

In a first series, performed without the dosage/applicator device, Kauczor et al. described findings with the new method in 8 healthy volunteers and 10 patients with lung disease [8]. Generally, the spatial resolution of  $^3\text{He}$ -MRI was judged to be better than that of ventilation scintigraphy even at this early stage of development. Lung parenchyma of healthy volunteers displayed an intense, homogeneously distributed  $^3\text{He}$  signal. In patients with chronic obstructive pulmonary disease (COPD) or pneumonia,  $^3\text{He}$  signal distribution appeared quite inhomogeneous. Space-occupying intrathoracic lesions or pleural effusions were associated with signal defects of a size apparently larger than that of lesions seen in the chest radiogram or CT image.

These early observations already suggested that  $^3\text{He}$  signal defects can represent both structural parenchymal defects and functionally dis-

turbed ventilation, e.g. in hyperinflated emphysematous regions or in areas of compression dystelectasis.

### Morphological studies

Morphological comparison of statically acquired  $^3\text{He}$  lung images in clinically healthy smokers vs. healthy non-smoking subjects showed a homogeneous high-intensity distribution of the signal in the lung parenchyma of non-smokers. In contrast, smokers' lungs showed 1–6 hypointense spots scattered between parenchyma containing high signal intensity (figure 2) [10]. Interestingly, Altes et al. demonstrated, in asthmatic patients, signal defects which were quite similar in location and size to those seen in our smokers; follow-up studies and bronchodilator challenges showed that these areas of regional hypoventilation varied in location over time and disappeared in response to bronchodilators [13]. Preliminary findings in our lung graft recipients demonstrate highly variable signal intensity distribution with multiple large hypointensities [14]. In native lungs these hypointensities may represent fibrosis or emphysema. In grafted lungs they may be non-specific correlates of bronchiolitis obliterans or infiltrates. Not infrequently, however, no structural correlates were detectable in the corresponding lung CT scans of these patients. This again points to the high sensitivity of the  $^3\text{He}$ -MRI method in detecting even small lung regions with ventilation impairment, but also its relatively limited ability to discriminate between structural and functional aetiologies.

### Dynamic studies of ventilation distribution

The – compared to conventional  $^1\text{H}$ -MRI – exceedingly strong  $^3\text{He}$  magnetisation (hyperpolarisation) may be utilised for very fast repetitive imaging protocols, i.e. to produce dynamic, movie-like imaging of cyclic respiration. Temporal resolution is currently of the order of 130 ms down to 30 ms/image. This makes it possible to establish

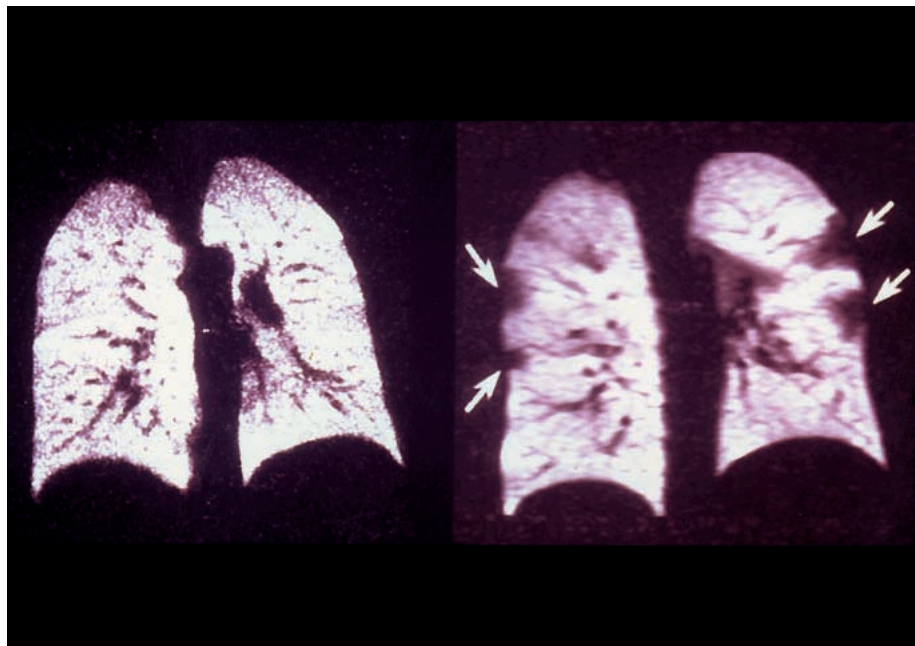
**Table 1**  
Experience of the  
Mainz  $^3\text{He}$  Group  
(2000).

Healthy subject studies		28
	Non-smokers	21
	Smokers	7
Patient studies		
Lung graft recipients		31
	Emphysema	12
	Pulmonary fibrosis	9
	Various aetiologies	10
COPD		8
Chronic thromboembolic pulmonary hypertension (CTEPH)		8
Other lung diseases		4
Total n		79

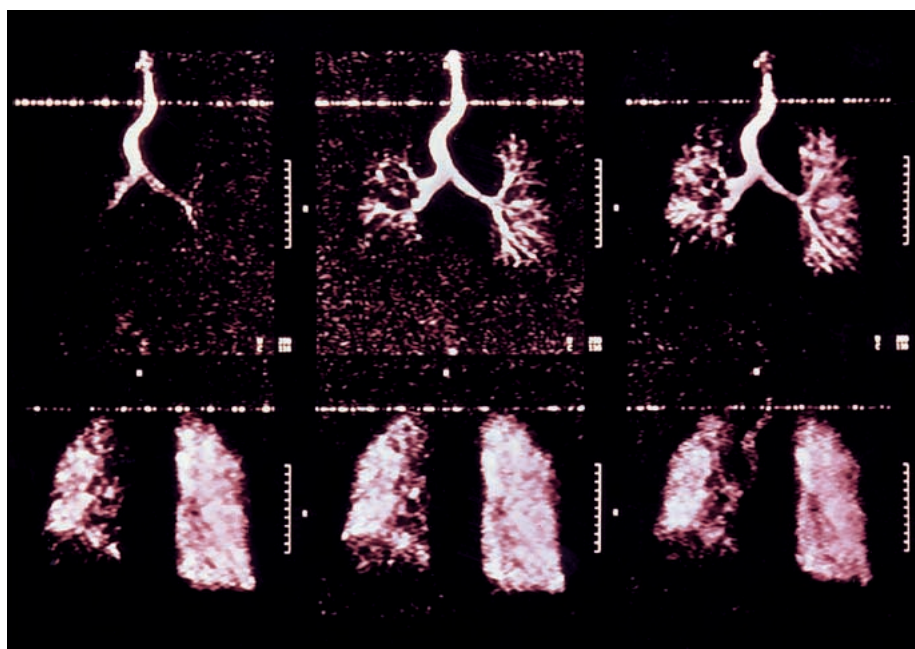


**Figure 2**

Pulmonary gas space morphology at  $^3\text{He}$ -MRI in two clinically healthy subjects. Left, nonsmoker; right, smoker (10 pack years); arrows: areas of lung parenchyma with reduced or absent  $^3\text{He}$  entry.

**Figure 3**

Fast dynamic  $^3\text{He}$  MR imaging (130 ms/image) of an inspiration (300 mL  $^3\text{He}$ ) in a patient with idiopathic pulmonary fibrosis (IPF) on the right and a well-functioning lung graft on the left [11]. Note delayed  $^3\text{He}$  entry into the native fibrotic lung (1<sup>st</sup> image) and premature emptying from this lung (last image).



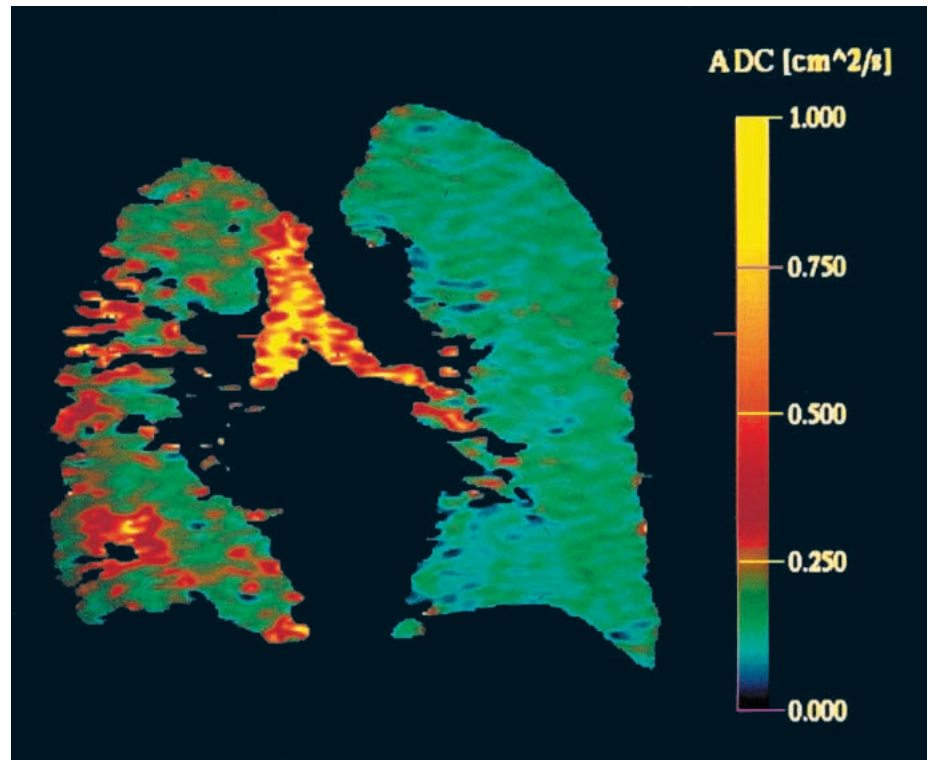
signal-time curves in the trachea and parenchymal regions and to compare lung regions with each other quantitatively, e.g. with regard to inspiratory filling and expiratory emptying (figure 3) [11, 15, 16]. First observations in our cohort show synchronous distribution into healthy volunteers' lungs, whereas in lung graft recipients inflow into fibrotic lungs and rejected grafts was typically delayed, with very heterogeneous signal distribution. Phase II studies are currently under way to explore the feasibility and potential of these techniques in obstructive and restrictive lung disease.

### Diffusion-weighted $^3\text{He}$ imaging

The unrestricted self-diffusion coefficient of  $^3\text{He}$  is  $\sim 2 \text{ cm}^2/\text{s}$ . In the lung, the diffusive movement of  $^3\text{He}$  atoms is restricted by bronchial and alveolar walls, to a degree which is dependent on the dimensions of the respective airspaces and the local gas composition. The use of so-called diffusion-sensitive MR imaging sequences allows determination and even mapping of "apparent diffusion coefficients" (ADC) of  $^3\text{He}$  (figure 4) [17]. The ADC in lung parenchyma is related to alveolar size, and has consequently been found to increase with age and in emphysema [18]. Consistent with these findings and (patho-)physiological expectations,

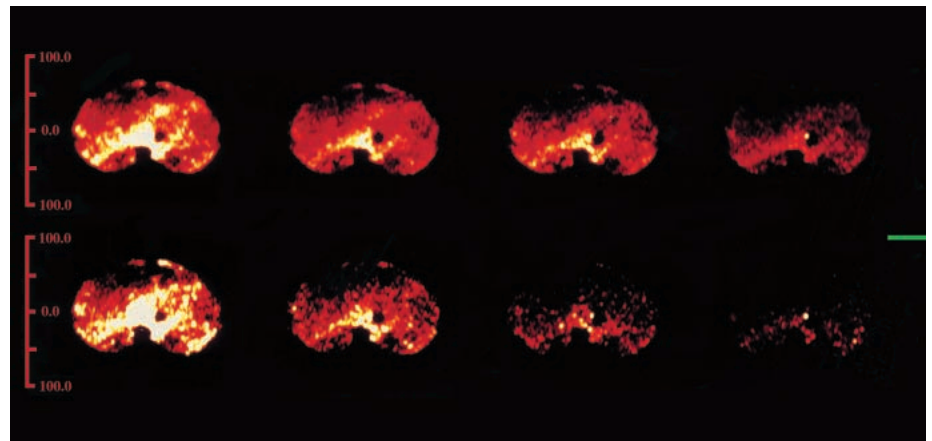
**Figure 4**

Diffusion-weighted  $^3\text{He}$  MRI: Pulmonary map of the "apparent diffusion coefficient" (ADC) in a patient with IPF on the right, and a well-functioning lung graft on the left (mod. from [17]). Note physiologically high ADC values in the tracheobronchial tree, homogeneity of ADC within the graft, as well as inhomogeneous and sometimes pathologically increased ADC in the native fibrotic lung.

**Figure 5**

Normal and accelerated decay of  $^3\text{He}$  signal intensity at normal ( $F_{\text{ET}}\text{O}_2 = 0.16$ ) and increased ( $F_{\text{ET}}\text{O}_2 = 0.35$ ) end-tidal (and hence, alveolar)  $\text{O}_2$  concentration in a porcine lung (transverse orientation).  $F_{\text{ET}}\text{O}_2$ , end-tidal fraction of oxygen.

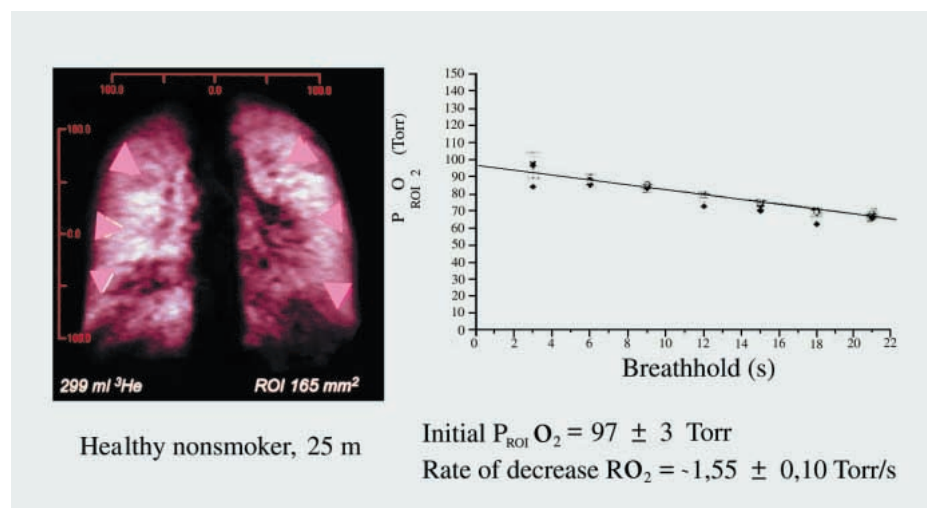
$F_{\text{ET}}\text{O}_2 = 0.16$



$F_{\text{ET}}\text{O}_2 = 0.35$

**Figure 6**

Left,  $^3\text{He}$  MR projection image of a healthy 25-year-old non-smoker, with regions of interest (ROIs) depicted for image-based  $\text{PO}_2$  measurement. Right, measured regional  $\text{P}_{\text{ROI}}\text{O}_2$  values and their decrease during breathholding. Note homogeneity of both  $\text{P}_{\text{ROI}}\text{O}_2$  distribution and rate of  $\text{P}_{\text{ROI}}\text{O}_2$  decrease. Image-based  $\text{P}_{\text{ROI}}\text{O}_2$  ranged between 94 and 101 mm Hg, measured end-tidal  $\text{PO}_2$  was 113 mm Hg.



ADC in the trachea was measured at  $0.67 \text{ cm}^2/\text{s}$ , in normal lung parenchyma between  $0.13$  and  $0.17 \text{ cm}^2/\text{s}$ , in functional lung grafts between  $0.15$  and  $0.18 \text{ cm}^2/\text{s}$ , and in fibrotic lungs with honeycombing between  $0.22$  and  $0.35 \text{ cm}^2/\text{s}$  [17].

### Image-based regional $\text{PO}_2$ -measurement in the lung

$\text{O}_2$  has paramagnetic properties and therefore, when mixed with hyperpolarised  $^3\text{He}$  in the alveolar space, destroys magnetisation at a rate proportional to local alveolar  $\text{PO}_2$  ( $\text{P}_{\text{AO}_2}$ ) [12]. This opens up a route to non-invasive determination of regional  $\text{P}_{\text{AO}_2}$ . Its influence can be extracted from  $^3\text{He}$  signal decay curves generated from appropriately timed image series, which are acquired during breathhold (figure 5) [19, 20]. In healthy subjects very homogeneous  $\text{PO}_2$  distribution was found with a mean in agreement with end-tidal  $\text{PO}_2$  measured at the mouth (figure 6). Since  $\text{P}_{\text{AO}_2}$  is the result of the local ventilation-perfusion ratio, this technique may develop into a quick, non-invasive and easily repeatable method of assessing ventilation-perfusion matching and estimating oxygen uptake from the lung.

### $^{129}\text{Xe}$ MRI: advantages and potential

Although the very first hyperpolarised gas MR images of the pulmonary airspace were produced with  $^{129}\text{Xe}$  [4], this hyperpolarised gas has since found its chief applications in NMR spectroscopic studies. The nuclear magnetic resonance frequency of  $^{129}\text{Xe}$  atoms is exquisitely sensitive to their chemical environment. Other characteristics, e.g. the longitudinal relaxation time constant which describes the decay kinetics of  $^{129}\text{Xe}$  hyperpolarisation, also vary depending on  $\text{PO}_2$ , haemoglobin and other local physicochemical parameters. Xenon is soluble in blood and tissues; hence, following inhalation, it equilibrates quickly, i.e. almost within one circulation time, with the blood volume and accumulates in highly vascularised organs (e.g. heart, brain). Consequently,  $^{129}\text{Xe}$ 's characteristic chemical shifting of its NMR spectrum from that of gas-phase  $^{129}\text{Xe}$  to that of  $^{129}\text{Xe}$  dissolved in plasma, lung tissue, red blood cells or brain allows analyses of  $^{129}\text{Xe}$  compartmental distribution and the kinetics of its exchange between these compartments. For such studies, e.g. into cerebral perfusion [21] or pulmonary  $^{129}\text{Xe}$  gas-tissue exchange and perfusion [22, 23], hyperpolarisation of the tracer gas is an elegant way of considerably enhancing the sensitivity of the NMR spectroscopic technique. In addition, the deoxyhaemoglobin and oxygen sensitivity of longitudinal relaxation and NMR spectral

peak position suggests that hyperpolarised  $^{129}\text{Xe}$  may become very useful in non-invasive MR-based measurement of blood and tissue oxygenation [24]. Beyond spectroscopy, both pulmonary gas-phase and dissolved-phase  $^{129}\text{Xe}$  imaging have also progressed within recent years [25–27], though not as rapidly as lung airspace imaging with  $^3\text{He}$ .

### Summary and perspectives

MRI of the lung using hyperpolarised noble gases – in particular  $^3\text{He}$  – as the signal source opens up new routes to imaging of airways and alveolar spaces with high spatial and yet unmatched temporal resolution. Diffusion-sensitive  $^3\text{He}$  MRI-techniques allow indirect assessment of bronchoalveolar dimensions by determining local apparent diffusion coefficients.  $\text{PO}_2$  sensitivity of  $^3\text{He}$ -magnetisation provides an image-based estimation of regional alveolar  $\text{PO}_2$  and  $\text{O}_2$  uptake into the blood. Hyperpolarised  $^{129}\text{Xe}$ , on the other hand, opens up a different and unique research field in spectroscopy, perfusion and oxygenation research in view of its lipid solubility and the chemical shifts of its NMR spectrum.

Currently,  $^3\text{He}$ -MRI is being assessed by several European and American research groups not only in animal models and human volunteers but already in patients (Phase II studies). First results have demonstrated the good imaging quality, reproducibility, feasibility and safety of the technique. Potential clinical applications are early detection and therapeutic monitoring of obstructive lung disease due to the sensitivity of  $^3\text{He}$ -MRI for small airway obstruction and air trapping. Another useful application may be pre- and postoperative regional lung function analysis in resective pulmonary surgery and lung transplantation. General advantages of  $^3\text{He}$ -MRI are avoidance of radiation exposure, the biochemical inertness of  $^3\text{He}$  and the nearly unlimited repeatability of studies, e.g. during follow-up of transplanted patients. Current limitations of the technique include the  $^3\text{He}$  production rate and the US and EU health authorities' still pending approval for clinical use.

---

#### Correspondence:

PD Dr. med. Balthasar Eberle

Klinik für Anästhesiologie

Klinikum der Johannes Gutenberg-Universität  
Mainz

Langenbeckstr. 1

D-55131 Mainz

E-Mail: eberle@anaesthesie.klinik.uni-mainz.de



## References

- Puybasset L, Cluzel P, Gusman P, Grenier P, Preteux F, Rouby J-J and the CT Scan ARDS Study Group. Regional distribution of gas and tissue in acute respiratory distress syndrome. I. Consequences for lung morphology. *Intensive Care Med* 2000;26: 857-69.
- Markstaller K, Eberle B, Kauczor HU, Aranda M, Bink A, Weiler N. Lung density distribution in dynamic CT correlates with oxygenation during pressure-controlled ventilation of pigs with lavage-ARDS. *Anesthesiology* 2000;93:B19.
- Happer W, Miron E, Schaefer S, Schreiber D, Van Wijngaarden WA, Zeng X. Polarization of the nuclear spins of noble-gas atoms by spin exchange with optically pumped alkali-metal atoms. *Phys Rev* 1984;A 29:3092-3110.
- Albert MS, Cates GD, Driehuys B, Happer W, Saam B, Springer CS, Wishnia A. Biological magnetic resonance imaging using laser-polarized  $^{129}\text{Xe}$ . *Nature* 1994;370 (6486):199-201.
- MacFall JR, Charles HC, Black RD, Middleton H, Swartz JC, Saam B, et al. Human lung air spaces: potential for MR imaging with hyperpolarized He-3. *Radiology* 1996;200:553-8.
- Kauczor HU, Hofmann D, Kreitner KF, Nilgens H, Surkau R, Heil W, et al. Normal and abnormal pulmonary ventilation: visualization at hyperpolarized He-3 MR imaging. *Radiology* 1996;201:564-8.
- Ebert M, Grossmann T, Heil W, Otten EW, Surkau R, Leduc M, et al. Nuclear magnetic resonance imaging on humans using hyperpolarized  $^3\text{He}$ . *Lancet* 1996;347:1297-9.
- Kauczor HU, Ebert M, Kreitner KF, Nilgens H, Surkau R, Heil W, et al. Imaging of the lungs using  $^3\text{He}$  MRI: preliminary clinical experience in 18 patients with and without lung disease. *J Magn Reson Imaging* 1997;7:538-43.
- De Lange EE, Mugler JP III, Brookeman JR, Knight-Scott J, Truwit JD, Teates CD, et al. Lung air spaces: MR imaging evaluation with hyperpolarized  $^3\text{He}$  gas. *Radiology* 1999;210:851-7.
- Günther D, Eberle B, Hast J, Lill J, Markstaller K, Puderbach M, et al.  $^3\text{He}$  MRI in healthy volunteers: preliminary correlation with smoking history and lung volumes. *NMR Biomed* 2000;13:182-9.
- Schreiber W, Weiler N, Kauczor H-U, Markstaller K, Eberle B, Hast J, et al. Ultraschnelle MRT der Lungenventilation mittels hochpolarisiertem Helium-3. *Fortschr Röntgenstr* 2000; 172:129-33.
- Saam B, Happer W, Middleton H. Nuclear relaxation of  $^3\text{He}$  in the presence of  $\text{O}_2$ . *Phys Rev* 1995;A 52:862-5.
- Altes TA, Powers PL, Knight-Scott J, Rakes G, Platts-Mills TA, De Lange EE, et al. Hyperpolarized  $^3\text{He}$  MR lung ventilation imaging in asthmatics: preliminary findings. *J Magn Reson Imaging* 2001;13:378-84.
- Lill J, Hanisch G, Markstaller K, Eberle B, Diergarten T, Buhl R, Kauczor HU.  $^3\text{He}$ -MRT bei Rauchern, Nichtraucher und Lungentransplantierten in Korrelation mit der Lungenfunktion. *Pneumologie* 2000;54:S3/4.
- Saam B, Yablonskiy DA, Gierada DS, Conradi MS. Rapid imaging of hyperpolarized gas using EPI. *Magn Reson Med* 1999;42:507-14.
- Gierada DS, Saam B, Yablonskiy D, Cooper JD, Lefrak SS, Conradi MS. Dynamic echo planar MR imaging of lung ventilation with hyperpolarized  $^3\text{He}$  in normal subjects and patients with severe emphysema. *NMR Biomed* 2000;13:176-81.
- Hanisch G, Schreiber W, Diergarten T, Markstaller K, Eberle B, Kauczor H-U, et al. Investigation of intrapulmonary diffusion by  $^3\text{He}$  MRI. *Eur Radiol* 2000;10 Suppl 1:S345.
- Brookeman JR, Mugler JP III, Knight-Scott J, Munger TM, De Lange EE, Bogorad PL. Studies of  $^3\text{He}$  diffusion coefficient in the human lung: age-related distribution patterns. *Eur Radiol* 1999;9:B21.
- Eberle B, Weiler N, Markstaller K, Kauczor H-U, Deninger A, Ebert M, et al. Analysis of intrapulmonary  $\text{O}_2$ -concentrations by magnetic resonance imaging of inhaled hyperpolarized  $^3\text{He}$ -lithium. *J Appl Physiol* 1999;87:2043-52.
- Deninger AJ, Eberle B, Ebert M, Großmann T, Hanisch G, Heil W, et al.  $^3\text{He}$ -MRI based measurement of intrapulmonary  $\text{PO}_2$  and its time course during apnea in healthy volunteers: first results, reproducibility, and current limitations. *NMR Biomed* 2000;13:194-201.
- Duhamel G, Choquet P, Grillon E, Lamalle L, Levie J-L, Ziegler A, et al. Xenon-129 MR imaging and spectroscopy of rat brain using arterial delivery of hyperpolarized xenon in a lipid emulsion. *Magn Reson Med* 2001;45:208-12.
- Ruppert K, Brookeman JR, Hagspiel KD, Driehuys B, Mugler JP III. NMR of hyperpolarized  $^{129}\text{Xe}$  in the canine chest: spectral dynamics during a breath-hold. *NMR Biomed* 2000;13:220-8.
- Venkatesh A, Hong KS, Kubatina L, Sun Y, Mulkern R, Jolesz FA, et al. Using dynamic hyperpolarized xenon MR to measure brain perfusion. *Proc Intl Soc Mag Reson Med* 2001;9:951.
- Bifone A. Perfusion imaging with hyperpolarized gases. *Eur Radiol* 1999;9:B39.
- Mugler JP, Driehuys B, Brookeman JR, Cates GD, Berr SS, Bryant RG, et al. MR imaging and spectroscopy using hyperpolarized  $^{129}\text{Xe}$  gas: preliminary human results. *Magn Reson Med* 1997;37:809-815.
- Swanson SD, Rosen MS, Coulter KO, Welsh RC, Chupp TE. Distribution and dynamics of laser-polarized  $^{129}\text{Xe}$  magnetization in vivo. *Magn Reson Med* 1999;42:1137-45.
- Ruppert K, Brookeman JR, Hagspiel KD, Mugler JP III. Probing lung physiology with xenon polarization transfer contrast (XTC). *Magn Reson Med* 2000;44:349-57.



## The many reasons why you should choose SMW to publish your research

### *What Swiss Medical Weekly has to offer:*

- SMW's impact factor has been steadily rising, to the current 1.537
- Open access to the publication via the Internet, therefore wide audience and impact
- Rapid listing in Medline
- LinkOut-button from PubMed with link to the full text website <http://www.smw.ch> (direct link from each SMW record in PubMed)
- No-nonsense submission – you submit a single copy of your manuscript by e-mail attachment
- Peer review based on a broad spectrum of international academic referees
- Assistance of our professional statistician for every article with statistical analyses
- Fast peer review, by e-mail exchange with the referees
- Prompt decisions based on weekly conferences of the Editorial Board
- Prompt notification on the status of your manuscript by e-mail
- Professional English copy editing
- No page charges and attractive colour offprints at no extra cost

### *Editorial Board*

Prof. Jean-Michel Dayer, Geneva  
Prof. Peter Gehr, Berne  
Prof. André P. Perruchoud, Basel  
Prof. Andreas Schaffner, Zurich  
(Editor in chief)  
Prof. Werner Straub, Berne  
Prof. Ludwig von Segesser, Lausanne

### *International Advisory Committee*

Prof. K. E. Juhani Airaksinen, Turku, Finland  
Prof. Anthony Bayes de Luna, Barcelona, Spain  
Prof. Hubert E. Blum, Freiburg, Germany  
Prof. Walter E. Haefeli, Heidelberg, Germany  
Prof. Nino Kuenzli, Los Angeles, USA  
Prof. René Lutter, Amsterdam, The Netherlands  
Prof. Claude Martin, Marseille, France  
Prof. Josef Patsch, Innsbruck, Austria  
Prof. Luigi Tavazzi, Pavia, Italy

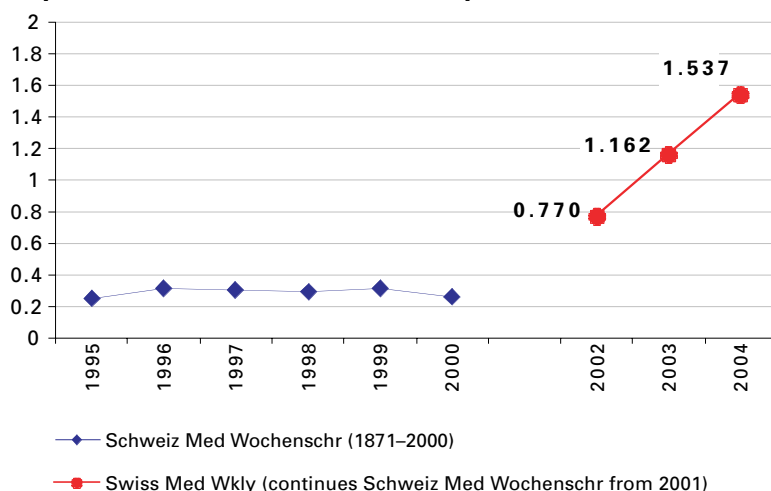
We evaluate manuscripts of broad clinical interest from all specialties, including experimental medicine and clinical investigation.

We look forward to receiving your paper!

Guidelines for authors:

[http://www.smw.ch/set\\_authors.html](http://www.smw.ch/set_authors.html)

### Impact factor Swiss Medical Weekly



**EMH**  **FMH**  
**SCHWABE**  
Editores Medicorum Helveticorum

*All manuscripts should be sent in electronic form, to:*

EMH Swiss Medical Publishers Ltd.  
SMW Editorial Secretariat  
Farnsburgerstrasse 8  
CH-4132 Muttenz

Manuscripts:	<a href="mailto:submission@smw.ch">submission@smw.ch</a>
Letters to the editor:	<a href="mailto:letters@smw.ch">letters@smw.ch</a>
Editorial Board:	<a href="mailto:red@smw.ch">red@smw.ch</a>
Internet:	<a href="http://www.smw.ch">http://www.smw.ch</a>